
Extracting the β -factor of a photonic crystal laser

Nanophotonics Theory and Signal Processing



Jonas Bach Olsen (s144099)

Frederik Diethelm Jacobsen (s144088)

Supervisors:

Andreas Dyhl Osterkryger

Weiqi Xue

Jesper Mørk

13th January 2016

1 Abstract

This project examines a photonic crystal laser with a triangular lattice crystal and a commercial semiconductor laser of the model FOL1404QQO to compare their β_{sp} -factors. This is done by comparing a simulation, based on numerical solutions of two coupled differential equations called the rate equations, and a series of experimental data.

Due to the many parameters in the rate equations, it was not possible to determine other factors than the β_{sp} -factor with certainty. These parameters have been estimated, but because of the many degrees of freedom, it was not possible to determine these accurately.

The experiments show a significant difference between the β_{sp} -factor of the two. The β_{sp} -factor of the photonic crystal laser being 10^4 times larger than the β_{sp} -factor of the commercial laser.

Contents

1	Abstract	0
2	Introduction	1
3	The Laser	1
3.1	Rate Equations	3
3.2	The Photonic Crystal Laser	5
3.3	The gain material	7
4	Method	7
4.1	Simulation of steady state solutions	8
4.2	Simulation of varying input power	9
4.3	Performing the measurements	11
5	Results of the simulation	12
5.1	The parameters' influence on the power output	12
5.2	Qualification of our estimates	15
5.3	Fitting simulation to data	16
6	Commercial Laser	17
7	Discussion of the results	19
8	Conclusion	20
	Bibliography	21
	Appendix A	22
	Appendix B	23
	Appendix C	24
	Appendix D	25
	Appendix E	27
	Appendix F	28
	Appendix G	34

2 Introduction

In recent years, interest in photonic crystal lasers has been on the rise, the relatively new field of nanophotonics has opened doors previously closed. This report explores a certain aspect of the photonic crystal laser, the so called β_{sp} -factor, a factor that describes how large a part of spontaneous energy decay of an excited system is translatable into photons that are directly usable by the laser system.

Ordinary lasers have an energy threshold which they need to pass for lasing to happen.

The benefit of the photons being supplied by spontaneous emission as opposed to them being supplied by stimulated emission, as it is usual in current lasers, is that it does not require the input power to be above this energy threshold value for them to be emitted. Ideally it would be possible to create a laser that relied solely on spontaneous emission to supply photons, thus eliminating the energy threshold of current lasers, while also reducing energy waste. To find the β_{sp} -factor, a simple simulation will be put together, relying on the formulas used to describe classic laser systems. This simulation will be fitted to measured data from a real photonic crystal laser. By comparing the simulation and the experimental data, we will be able to estimate the β_{sp} -factor of the laser.

3 The Laser

Laser is an acronym for "light amplification by stimulated emission of radiation". [2] A laser is a light source that emits light at a single wavelength, phase and direction.

A laser is made up of two major components. A carrier reservoir, which is made of a material with internal energy levels whose energy difference correspond to the energy of the photons of the laser. This material is pumped by an energy source, and the decay of it is the source of the photons that are ultimately the laser output. The other major component being the photon reservoir, a contained space between two partially reflective surfaces which contain the photons of the system. The carrier reservoir is always confined to a smaller spatial volume than the photons. Both reservoirs are placed between two mirrors, as the configuration shown in Figure 1.

In the carrier reservoir, the carriers, usually electrons, are "pumped", meaning energy is added to the reservoir and electrons are either added to the conduction band of the semiconductor or pumped to an excited state. The carriers, once in the reservoir, will decay from the conduction band into the valence band. This transition can happen in several different ways, with different kinds of energy emissions as a result. The first kind of transition is the spontaneous emission. This occurs randomly and each decaying electron will release a photon with energy corresponding to the difference between the conduction band and the valence band as shown in Figure 2a. However the phase and direction of the emitted photons are random.[4]

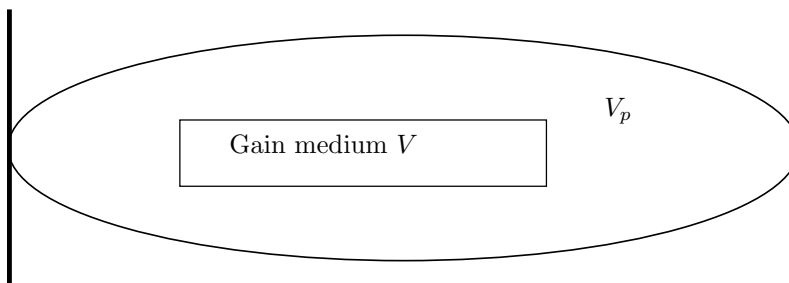


Figure 1: A model showing the gain medium within the laser cavity. The gain medium has a volume of V and the carriers reside within. The remaining volume V_p is the photon volume. When the photons pass through the gain medium, there is a possibility of a stimulated emission to occur. Letting the volume of V be close to the volume of V_p increases the amount of time in which stimulated emission can occur.

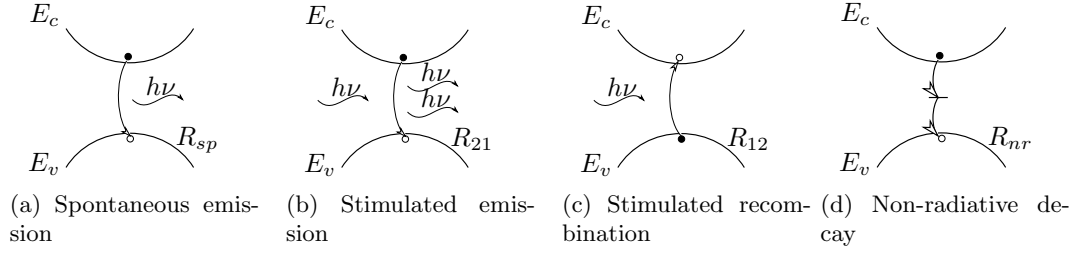


Figure 2: The carriers can decay in different ways. The kind of decay which enables is the stimulated emission. However, with an increasing β_{sp} -factor, the spontaneous emissions become increasingly important.

The second kind of transition is the stimulated emission. As hinted by the acronym of laser, this is the important part! Stimulated emission happens when a photon passes close by a carrier in the valence band, and thus making it decay by emitting a photon in the same phase as the passerby. The important part of this kind of decay is that the photon pairs will have the same direction and phase. By placing the carrier reservoir between two mirrors, as shown in Figure 1 it is possible to cultivate this kind of emission. This is the goal of the whole setup, as the stimulated photons make up most of the emitted light. This process is shown in Figure 2b.[4]

The final kind of decay is the nonradiative decay, this kind of decay is usually caused by impurities in the carrier reservoir which create additional possible energy levels between the conduction band and the valence band. This causes the decay to happen in steps, and emit energy in phonons, or heat, instead of photons. This process is shown in Figure 2d.[4]

Figure 3 shows the process of lasing from start to end. The rate of electrons added to the system per second is described by I/q , with an efficiency coefficient η_i to take the injection losses into consideration.[4]

From the carrier reservoir with a volume of V and a carrier density N , the rates of the different kinds of decay are described by their decay-rates, given by the carrier density divided by the respective lifetimes. Thus the rate of spontaneous emission is given by

$$R_{sp}V = \frac{N}{\tau_{sp}}V, \quad (3.1)$$

where R_{sp} is the spontaneous decay rate per volume, and τ_{sp} is the spontaneous emission lifetime. The nonradiative emission is given by

$$R_{nr}V = \frac{N}{\tau_{nr}}V, \quad (3.2)$$

where R_{nr} is the non-radiative decay rate per volume, and τ_{nr} is the non-radiative lifetime. [4] The non-radiative decays are unimportant for this report as the energy they produce is dissipated. In addition their rate is usually relatively low compared to the other kinds of decay. The spontaneous decay that add to the photon reservoir is the part, which by chance have the same direction, phase and polarisation as their stimulated counterparts. This is described by $R'_{sp}V = \beta_{sp}R_{sp}V$, where β_{sp} is the fraction of the spontaneously emitted photons that have the right direction, phase, and polarisation and therefore add to the photon reservoir.

The main process of stimulated emission is shown as $R_{21}V$ in Figure 3, where it is the amount of carriers able to decay by stimulation. This is a self-perpetuating process. As time goes on, more of the lasing will come from the stimulated emission and be in the same phase, until an equilibrium has been reached.

However, some of the photons will be absorbed, and make the energy go back to the carrier reservoir. It is counterproductive, but is a natural consequence of the setup seen in Figure 2c.

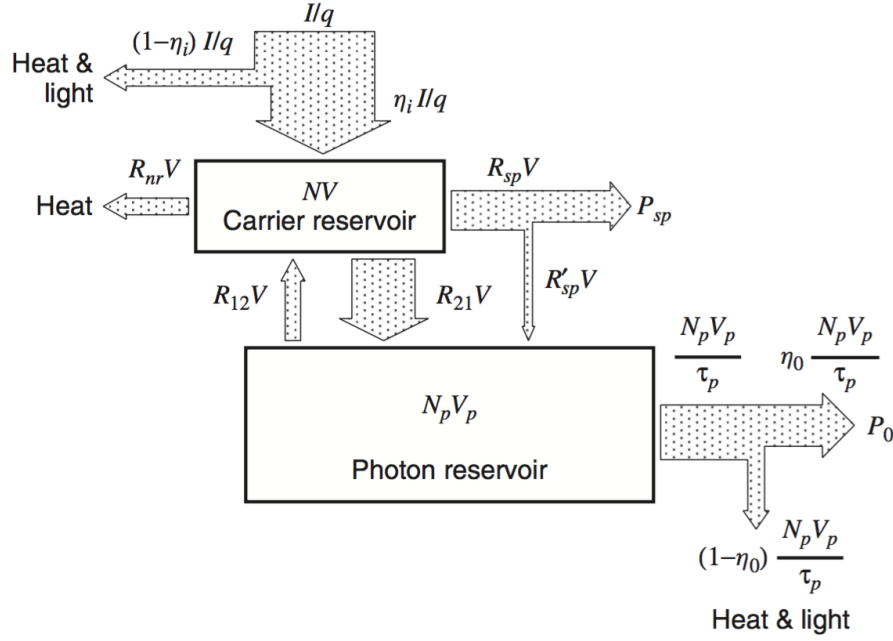


Figure 3: Sketch showing the process of lasing. As the carriers travel through the different steps of lasing, energy is lost in many different ways. The figure visualise these losses. [4]

Once a photon has arrived at the photon reservoir, it will be mirrored back and forth until it passes through the mirror and is emitted as power.

The process of lasing itself depends on how large a part of the photons pass through the mirrors on each roundtrip, the collected "loss" is shown in Figure 3 as

$$\frac{N_p V_p}{\tau_p}, \quad (3.3)$$

meaning it depends on the total amount of photons of the right phase and wavelength in the reservoir, and the average lifetime of the photons in said reservoir.[4]

To get the actual lasing output, shown as P_0 in Figure 3, we have to take other losses into account, including losses from transmission through the mirror such as scattering and absorption. This efficiency is named η_0 in Figure 3. [4]

3.1 Rate Equations

The rate of transition from input to output can be described by two coupled differential equations called the rate equations. The rate equations encompass all the transitions shown in Figure 3 and look as follow:

$$\frac{dN}{dt} = \frac{\eta_i I}{qV} - (R_{sp} + R_{nr}) - v_g g N_p, \quad (3.4)$$

$$\frac{dN_p}{dt} = \left[\Gamma v_g g - \frac{1}{\tau_p} \right] N_p + \Gamma R_{sp} \beta_{sp} \quad (3.5)$$

Eq. 3.4 describes the rate at which the carrier density N changes, at an input current I . The first term of the equation, $(\eta_i I)/(qV)$, describes the change in the rate at which the carrier density changes as a result of the input current, taking the injection efficiency into account, meaning that only $\eta_i I$ of the initial input actually arrives to the system. Thus $(\eta_i I)/q$ describes the number of

carriers created, and since the equation describes a carrier density, this is again divided by the carrier reservoir volume V .

The rates $-(R_{sp} + R_{nr}) = -(N/\tau_{sp} + N/\tau_{nr})$ describe losses in carrier density to spontaneous and nonradiative decay, dependent on the carrier density N and the spontaneous and nonradiative lifetimes τ_{sp} and τ_{nr} .

The final term of Eq. (3.4) is the part that describes the carrier loss to stimulated emission, $v_g g N_p$. This is modelled by the gain factor g , which describes how many photons per length are created by stimulated emission, and the group velocity v_g , which describes the group velocity through the medium. This combined with the photon density N_p gives the speed of the stimulated transition. The gain g can be modelled by [1]

$$g = \frac{g_0}{1 + \varepsilon N_p} \ln \frac{N}{N_{tr}} \quad (3.6)$$

In Eq. (3.6) g_0 and ε are material factors dependent on the gain material, N_{tr} is known as the transparency density, given that when $N = N_{tr}$, $\ln \frac{N}{N_{tr}}$ will be 0 and thus there will be no gain. When $N < N_{tr}$ the gain will be negative, and there will be no stimulated emission. Only while $N > N_{tr}$ will g be positive, and stimulated emission will happen.

Eq. (3.5) describes how quickly the photon density N_p changes. The term on the right hand side, $\Gamma v_g g N_p$, directly mirrors the last term of Eq. (3.4), since "losses" to stimulated emission in the carrier reservoir directly translate to gain in the photon reservoir. The difference between the last term of Eq. (3.4) and the first term of Eq. (3.5), is the form factor Γ defined by the relation between the volume of the carrier reservoir and the volume of the photon reservoir,

$$\Gamma = \frac{V}{V_p} \quad (3.7)$$

This describes that the photon density will only increase through stimulated emission as long as the photons are within the gain area. The second term of the equation, N_p/τ_p , is the rate of loss of photons. This is where the final output of light stems from, as mentioned earlier this is given by the density of photons divided by the photon lifetime τ_p . [4]

The final term of Eq. (3.5), $\Gamma R_{sp} \beta_{sp}$, is the gain from the spontaneous decays of carriers, which has the same phase and direction as the stimulated light. As mentioned in Eq. (3.3) this can be found by the β_{sp} th part of the spontaneous emitted light. The gain rate of this is given by $\Gamma R_{sp} \beta_{sp}$ where Γ plays the same role as in the first part of Eq. (3.5). The photon gain rate from the β_{sp} factor is usually insignificant compared to the gain rate from the stimulated emission in classical lasers.

Eq. (3.4) and Eq. (3.5) are as earlier mentioned two coupled differential equations. After some time these equations will reach an equilibrium. There is one net positive part of these equations, the $\eta_i I(qV)$ term. As long as the power is a set value, this is constant. On the other hand the negative terms will continue to rise with the carrier density, until they eventually reach an equilibrium where

$$\frac{dN}{dt} = \frac{dN_p}{dt} = 0. \quad (3.8)$$

At this stage the laser is at a steady state. This means that the carrier and photon densities both depend on the initial pumping power. When these steady states are reached the gain and the carrier density will stabilise at certain values, dependent on the initial power input after which stimulated emission will add to the photon reservoir.

The power input required to reach this point is dubbed I_{th} , for I at threshold. After this value is reached, the gain value g and the carrier density N will stabilise at values called the gain at

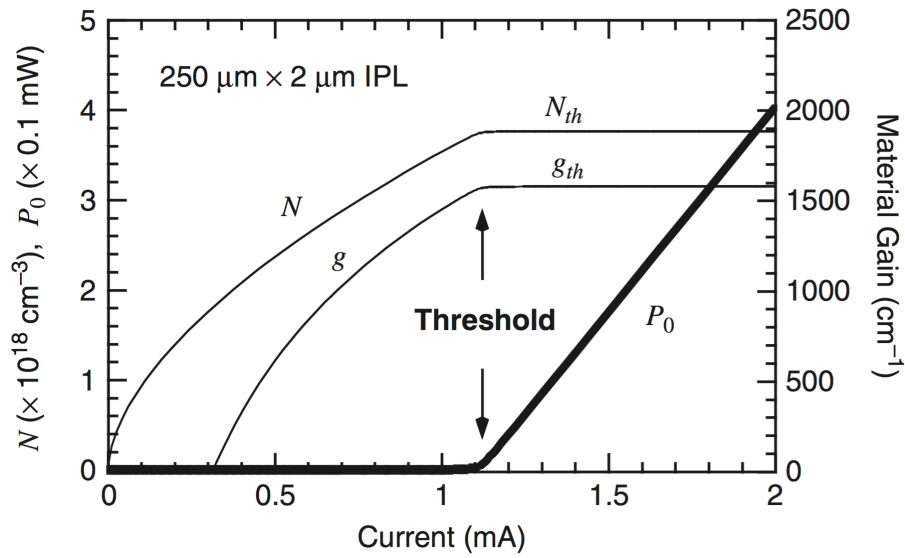


Figure 4: The plot shows the carrier density, gain and output power as a function of input current. The threshold clearly shows that the carriers and gain stop increasing once the threshold has been reached, however the lasing starts at this point. [4]

threshold g_{th} , and carrier density at threshold N_{th} . Although the photon density N_p will increase if the power input is increased further. These values are very important, since lasing will only occur after the power input passes I_{th} . After this point the dominant way of transmission will be stimulated emission, and the photon density N_p will rise rapidly with any further power increase, and thus the final output will too. This process is shown in Figure 4. [4]

3.2 The Photonic Crystal Laser

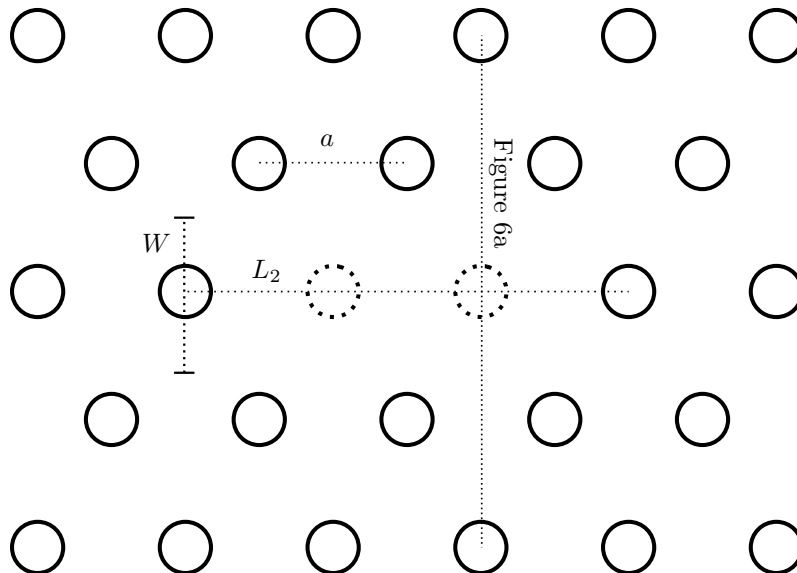


Figure 5: Triangular photonic crystal unit cell. Two holes have been removed, shown by the stapled circles. This cavity has the length L_2 . The length of the cell unit a is also shown. Lastly, the view of the crystal in Figure 6a can also be seen in the figure.

There are a number of ways to make the the reservoirs of a laser and one of them is to use a

photonic crystal. A photonic crystal laser is in many ways just another laser. It has a threshold, pump, output, reservoirs and many of the other characteristics of a laser. The big difference is the structure of the cavity and the consequences of this.

To describe a photonic crystal laser, we start by looking at a plate, and remove columns down through it, in a triangular crystal unit-cell shape. A two-dimensional view of this plate from above can be seen in Figure 5. Air columns are sketched as solid circles.[3] The lattice constant a describes the distance from the center of one column to the next. If we now “remove”, or avoid making, a number of columns in a line, as can be seen by the stapled circles in Figure 5, we now have a cavity with length L_n , where n is the number of columns removed in a line.

The reason photonic crystals can be used to create lasers, is caused by an interesting attribute of the photonic crystal. It has a photonic bandgap for some polarizations, as shown in Figure 7. This means that only photons with frequencies and wavenumbers placing them inside the photonic band gap can exist inside the photonic crystal. By making the aforementioned structures in the crystal it is possible to make it so there is no bandgap outside the cavity, thus the ends of the cavity itself will act as a mirror, since the light can not exist outside of the crystal. This is caused by the refractive indexes of the structure causing all light outside of the cavity to have destructive interference with itself. [3] That being said, not all polarizations have a photonic bandgap. If we view the photons relative to the photonic crystal, like in Figure 6a, with the z -axis being the direction the light propagates, the transverse electric and magnetic waves will be defined as being:

$$\text{TE : } E_y, B_x, B_z, \quad (3.9)$$

$$\text{TM : } B_y, E_x, E_z. \quad (3.10)$$

The polarization is very important, since only the TM waves have a photonic bandgap for a triangular lattice photonic crystal, as shown in Figure 7, thus only TM waves will be present in the reservoir.

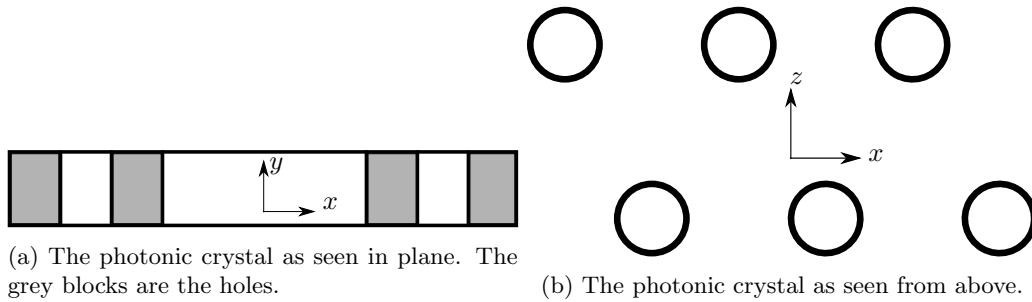


Figure 6: The coordinate systems used to describe the TE and TM modes in Eq. 3.9 and 3.10.

Having some modes being impossible in the cavity, increases the ratio of usable photons in cavity from spontaneous emission, and thereby increasing the β_{sp} factor, compared to the usual laser! [3] The more columns missing, the bigger the cavity becomes. By examining the geometrical symmetries of the triangular unit cells, the length can be shown to be

$$L_n = (1 + n)\sqrt{3}a \quad (3.11)$$

where n is the number of missing columns.

The width of the cavity is a bit tougher to calculate, and there is no definitive definition as to how to calculate it. We have made an attempt to define it, as can be seen in Figure 5. The width will be used as an average between the smallest and largest width. The smallest is a , and the largest is L_1 as shown in Figure 5;

$$W = \frac{\sqrt{3} \cdot 3}{2} a \quad (3.12)$$

Keep in mind that these values are only approximations, as the limits of the photon cavity is not as sharply defined in a real photonic crystal laser.

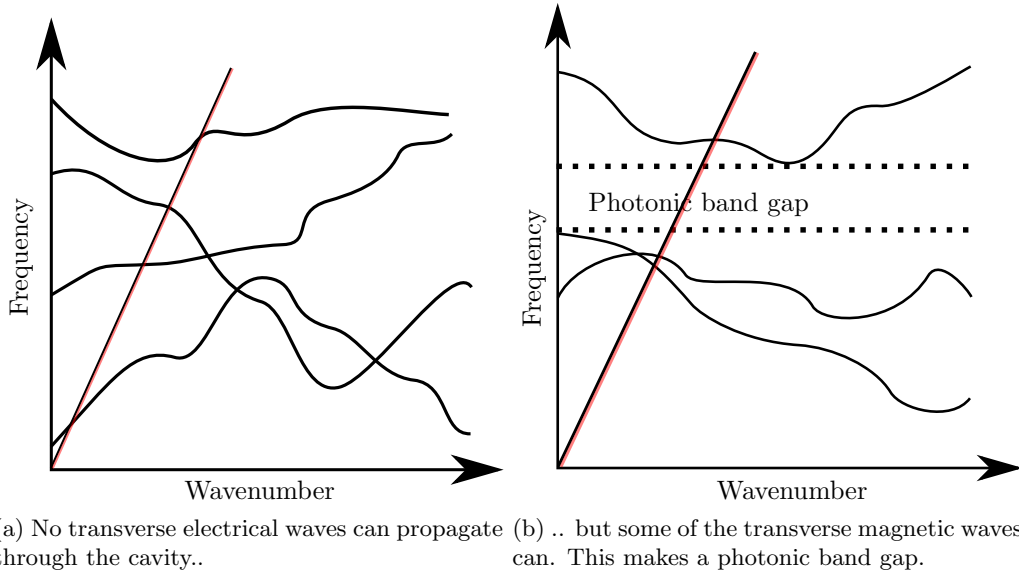


Figure 7: Example of the allowed modes for the electrical and magnetic waves in the cavity. All light in the area left of the red lines exist in empty air, making it dissapate quickly from the crystal.

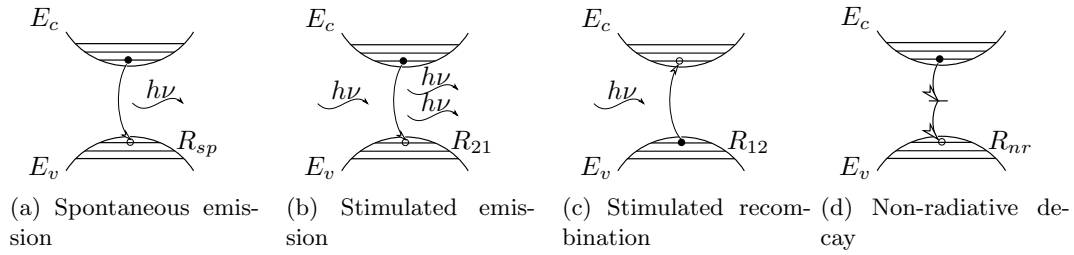


Figure 8: Quantum dot decays, only decays from line to line are possible

3.3 The gain material

In section 3 it was discussed how a laser functions in broad terms, however lasers using quantum dots as gain material of a photonic crystal laser work slightly differently. In most commercially used lasers, such as the one described in section 3, a semiconductor is used as gain medium, this can be seen in Figure 2 where the possible energy levels for the conduction and valence band both are continuous. In contrast to this we use quantum dots as gain material in our photonic crystal laser experiment. These are geometrically so small that they only allow certain wavelengths, since only certain combinations of standing waves are possible. This means the possible energy levels of the conduction- and valence band are discrete, as shown in Figure 8.

Theoretically this means the β_{sp} -factor will be significantly larger than a laser using a semiconductor as a band gap. This is caused by there being less possible alternative ways the gain material can decay, thus more of the spontaneous decay will correspond to the lasing phase and wavelength.

4 Method

While we would like to find the β_{sp} factor, it is not easily done. Through an experiment we will take measurements of varying input power and find the output power. The experiment has many factors of efficiency, and there is no easy way to measure the parameters we would like to find. To test the laser, we therefore make a simulation of a laser and try to fit it to measurements of the photonic crystal laser of the experiment. Finally, we try to simulate a laser undergoing a varying input power, and see what consequences this has on the carrier and photon densities.

4.1 Simulation of steady state solutions

In this first simulation, the attempt is to create a simulation where it is easy to compare the simulation to the experimental data, through varying the parameters. Because of the small time scales and the time it takes to take a measurement, we look at steady state solutions. This means we solve the rate equations in Eq. (3.4) and Eq. (3.5) for their steady state solutions, isolate the input current I and the photon density N_p to arrive at the following two equations:[4]

$$I(N) = \frac{qV}{\eta_i} (N/\tau_{sp} + N/\tau_{nr} + v_g g(N) N_p(N)), \quad (4.1)$$

$$N_p(N) = \frac{\Gamma \beta N / \tau_{sp}}{1/\tau_p - \Gamma v_g g(N)}. \quad (4.2)$$

Since we measure the input as a function of power, we would like to paraphrase Eq. (4.1) to describe the power instead of current. This is done by realizing that every electron going into the pump will become a photon with a specific efficiency (still η_i). This photon will have an energy determined by $h\nu$, and we can therefore realise that

$$\frac{I}{q} = \frac{P_{in}}{h\nu}. \quad (4.3)$$

However, our output power is not listed in the steady state solutions either, but we expect it to be proportional to the photon density (double the amount of photons, double the power). Also, it should be inversely proportional to the lifetime of the photon τ_p . If the photon is less time in the cavity, the power will increase. But what does the photon lifetime depend on? A fair approximation for it can be extracted from the steady state solution for the rate equation for photon density, Eq. (3.5). This approximation relies on the β_{sp} -factor being small enough to be negligible, which leaves us with: [4]

$$0 = \Gamma v_g g N_p - \frac{N_p}{\tau_p} \quad (4.4)$$

If we solve for τ_p at the threshold gain g_{th} , where the generation and recombination of photons are equal to each other, we get the approximation

$$\frac{1}{\tau_p} = \Gamma v_g g_{th}. \quad (4.5)$$

In addition, the photon lifetime can also be given by [4]

$$\frac{1}{\tau_p} = v_g (\alpha_m + \langle \alpha_i \rangle), \quad (4.6)$$

where α_m is the mirror loss and $\langle \alpha_i \rangle$ is the average internal loss.

Each time a photon reaches a mirror, it will have a chance to be reflected or be transmitted. If the photon hits the mirror more times per unit time, its lifetime will decrease. But if we increase the time in which the photons can create new photons through stimulated emission, by increasing the Γg_{th} factor, the photon lifetime will also decrease. But Eq. (4.5) is not complete. It is deduced from the rate equations and assuming $\beta_{sp} = 0$. As we will later see, this is not always a good estimate, and the lifetime of the photons become more complicated.

These two observations can be used to describe the output power. In fact, it can be described by the equation [4]

$$\eta_0 V v_g g_{th} N_p = \frac{P_0}{h\nu}, \quad (4.7)$$

where η_0 is the output efficiency, describing all the losses the output goes through until it is collected. This includes losses in the cavity, mirrors, photons not hitting the detector and various other factors.

Therefore from Eq. (3.4), the steady state equation for the current, can be rewritten into

$$P_{in}(N) = \frac{hc}{\lambda} \frac{V}{\eta_i} (N/\tau_{sp} + N/\tau_{nr} + v_g g(N) N_p(N)) \quad (4.8)$$

to get an expression for P_{in} solely dependent on N . In addition to this, we use the model for gain, Eq. (3.6), to describe $g(N)$.

To numerically solve these equations, we start by defining a vector N with the dimension h_1 , running from an arbitrary (but relevant) starting value, to the threshold N_{th} . For each value of N , the corresponding value of g , N_p and P_{in} are calculated.

We now raise the power, with a lot of steps, to three times the current power, or three times the threshold. For each step, the photon density is calculated by using

$$N_p = \Gamma \frac{N}{\tau_{sp}} \beta_{sp} \tau_p \quad (4.9)$$

before the threshold when there is no stimulated emission, and

$$N_p = N_{p,th} + \frac{P - P_{th}}{h\nu \cdot V v_g g_{th}} \quad (4.10)$$

after the threshold. In Eq. (4.10) $N_{p,th}$ is the value of Eq. (4.9) at P_{th} . To convert this to the power, we use Eq. (4.7). Finally, we can plot the output power as a function of input power.

The script described in this section can be seen in Appendix A.

4.2 Simulation of varying input power

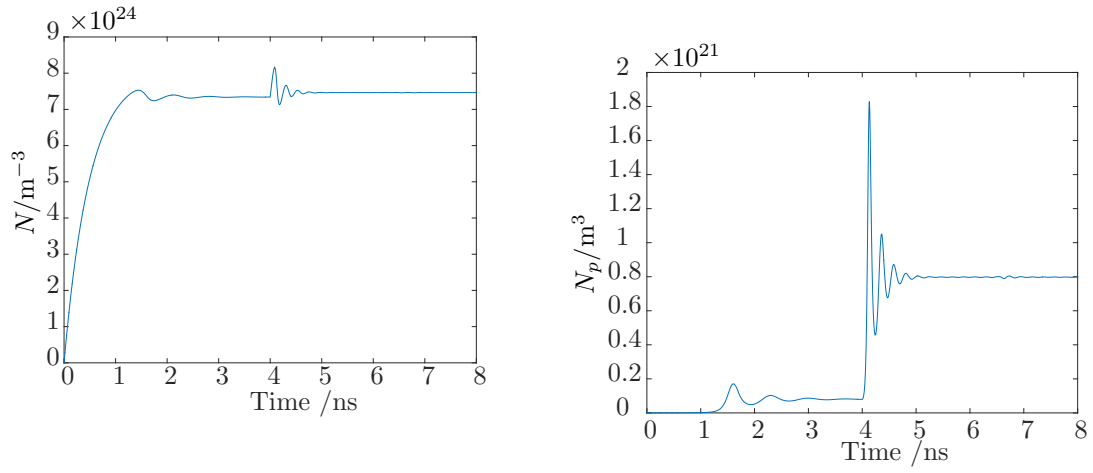
To see how the carriers and photons in the reservoirs depend on the time during the steady states, we will simulate a changing pump power, and plot the output as a function of time.

To do this, a script is created which uses the rate equations to simulate the carrier and photon densities. This script can be seen in Appendix D, and uses the built-in ode45 function in matlab. This function solves the differential equation numerically. The way the script simulates a varying input current is by starting out with almost empty reservoirs, run it for a few nanoseconds with a constant current just above I_{th} and then turn the current up to twice the threshold. The simulation is now run again, with the final values from the first part of the simulation.

Once the simulation has run for both current inputs, the data is plotted. The carrier density can be seen in Figure 9a, the photon density in Figure 9b, and the gain can be seen in Figure 10. One of the interesting things about these figures, are the oscillations. The carriers do not reach their steady state instantaneously, but oscillate. It takes some time before any photons even appear in the cavity.

To try to understand the oscillations, we have to look at what the gain actually is. The gain in the simulation is modelled by Eq. (3.6), and has the unit m^{-1} .

The simulation starts with a very low amount of carriers and photons in the reservoirs, so the gain can function. The gain is a way to describe how many stimulated emissions occur per length. At the start, the relation N/N_{th} is very small, and the gain is therefore negative. Once the injection has taken place for a short time, the carriers will be in abundance, and stimulated emission begins



(a) Carriers with varying input current. Because the current is above the threshold, the carriers will reach an equilibrium which is independent from the input current. The additional energy added through the additional current will increase the photon density.

Figure 9: Simulation of the carrier and photon densities. The current is at $1.1 \cdot I_{th}$ up to 4 ns and is then turned up to $2 \cdot I_{th}$.

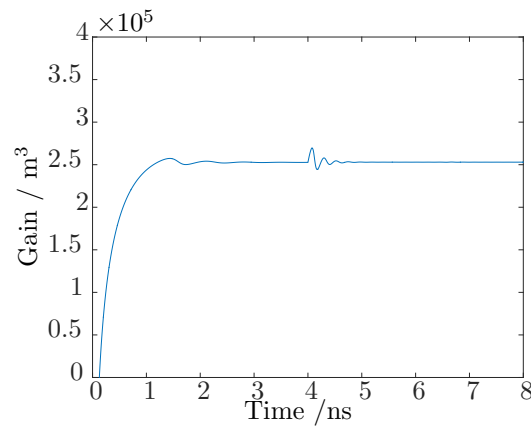


Figure 10: Gain as a function of time with varying input current. The input current is the same as in Figure 9, since both values are above I_{th} the gain becomes a constant.

to take place. Once the equilibrium is reached and the current is constant, the carriers are at a threshold, N_{th} . This situation can be seen in Figure 11a. We also notice that the gain is constant once the carrier threshold has been reached.

The injection current is now turned up to $2 \cdot I_{th}$ and the carriers spike. The situation can be seen in Figure 11b. This increases the carrier density for a short time. Because the photon density has not had time to make stimulated emissions, the photon density does not change for a short time. With the spiking carrier density, the gain will change. At this point, our carrier reservoir is filled, but the gain is also at its maximum (the small spike at $t = 4$ ns in Figure 10). The carriers will now undergo stimulated emission. With the carrier reservoir full, each emission will cause more emissions. This will cause a temporary runaway effect, as the mirrors will not be able to emit the light faster than more photons are emitted by stimulated emissions. This situation can be seen in Figure 11c.

However, this will not be able to keep going. and the carrier reservoir will be emptied, and the photons will be emitted through the mirrors. With fewer photons in the reservoir, the injection has a chance to fill up the carrier reservoir again. The few photons left will spike up again, and the carriers will decay again, however not as extreme as the first time. After a few oscillations, the carrier and photon densities will reach an equilibrium.

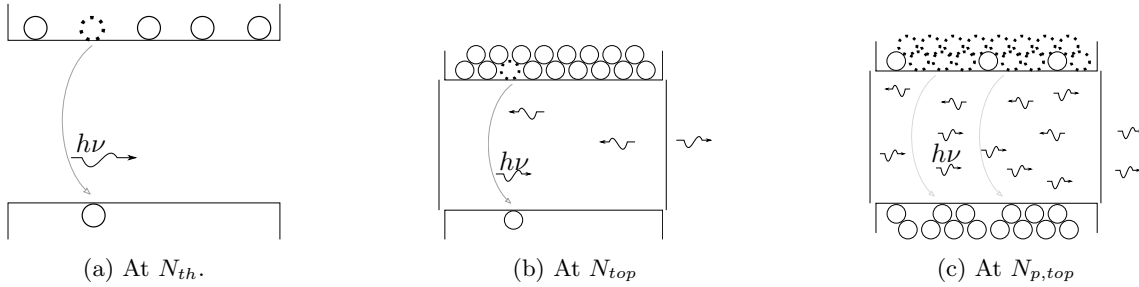


Figure 11: Different situations for places on the varying current. The situations describe the peaks in Figure 9.

4.3 Performing the measurements

The laser used to make these measurements is an optically pumped photonic crystal laser using quantum dots as gain medium, with a center to center distance, a of 48nm and a cavity length of L10. The given specifications for this setup can be seen in Appendix G.

The experimental setup can be seen in Figure 12. The lines between each device is an optical fiber. The initial input is produced by a pumping laser at ①. The light produced is 1480 nm. The light travels onto ②, which is an attenuator, used to vary the intensity of the pumping light. Since λ

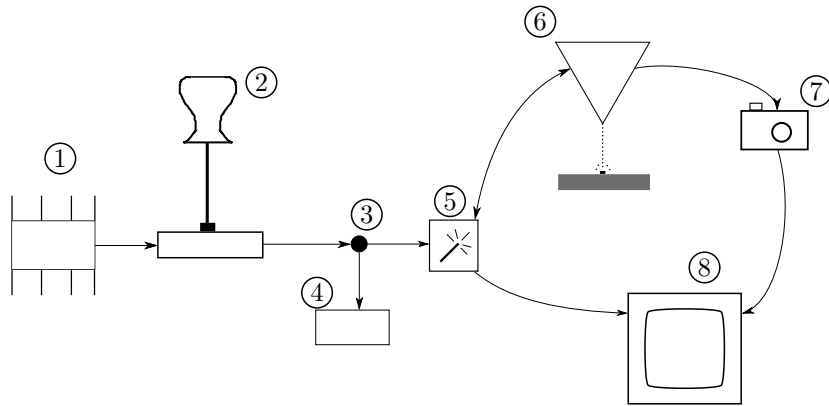


Figure 12: The experimental setup used to take the measurements for the photonic crystal laser.

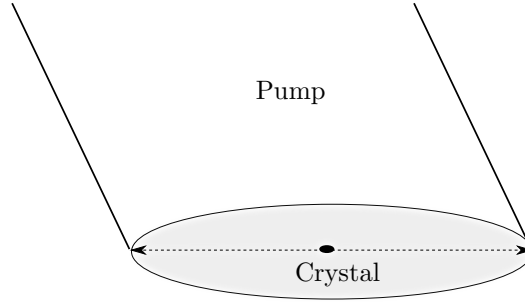


Figure 13: The pump beam has a larger area (grey) than the photonic crystal (black dot in the center).

depends on the current, it is favourable to keep it constant, and instead vary the amount of the laser let through.

The laser now continues onto ③ which is a beamsplitter, splitting the laser into a 99-to-1 ratio. The one percent goes ④, a powermeter. The last 99 percent goes to ⑤. Here, the laser (the first time it passes through) goes on to ⑥, which is where the photonic crystal is. This crystal is quite small, compared to the laserbeam. There is an injection efficiency related to the area ratio, which is shown in Figure 13. The light also has to be absorbed which only happens with an efficiency at about 0.002. Because of the gain material, the photons in the crystal will have less energy and so a longer wavelength. This is used when the photons are emitted from the crystal, absorbed by a detector and go back through the *same* fiber from which they came from. Back in ⑤, a "wave guide" will split the light depending on wavelength. The light at $\lambda = 1510$ nm, from the photonic crystal laser, will go on to ⑧, while the higher energy light will still go to ⑥.

At ⑧ the light will be analysed, as can be seen in Figure 14. A few modes can be seen, but we choose to focus on the tallest one. In this dataset, it is the spike at about 1590 nm. This dataset is only an example, and the wavelength is different for the simulation. To find the output power of the photonic crystal laser, we read the tallest peak's power, which is in dBm, and convert it to watts with

$$P_{out} = 10^{\frac{P_{dB}}{10}} \text{ .mW} \quad (4.11)$$

All the data points are now analysed through a script in matlab see Appendix C. In short, we make a list of the power measured at the power meter in Figure 12 and multiply by 100 to find the power going to the crystal. The script then loads each data set, one of which can be seen in Figure 16, finds the maximum and transforms it to the power using Eq. (4.11). Before transforming, it will deduct the total transmission loss, 6 dB. The results from the L_{10} laser can be seen in Figure 15.

5 Results of the simulation

With the many parameters used in the simulation, and each with an impact on the output power, we need to take a closer look at each one of them. What does it mean to increase the β_{sp} -factor? What happens when the group velocity is changed?

Afterwards, we will explain our guesses and starting points on some parameters. In the end, we will try to make the simulation resemble the measured data as closely as possible.

5.1 The parameters' influence on the power output

As mentioned in section 4 this simulation compares an initial power input in watts, P_{in} , with a final power output, P_{out} . In this simulation it is possible to tweak a number of different parameters. In

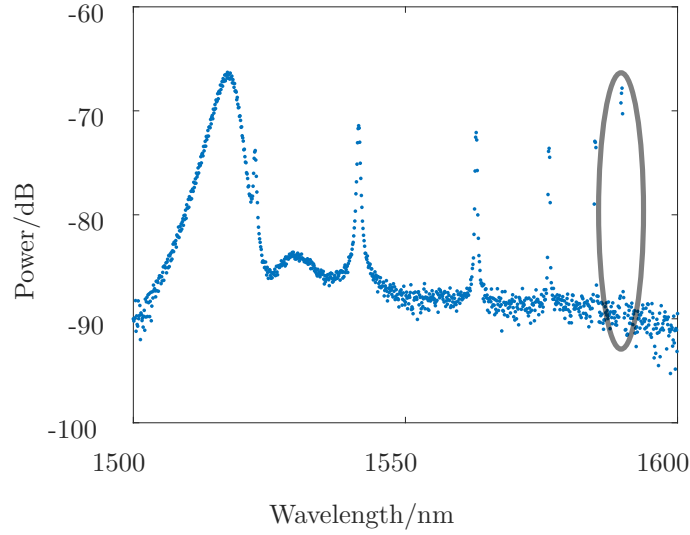
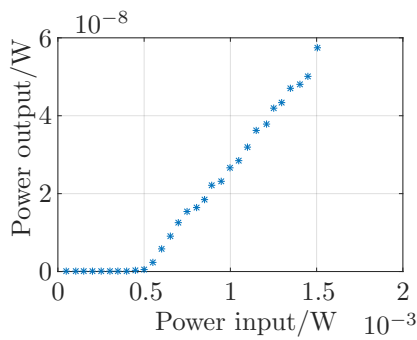
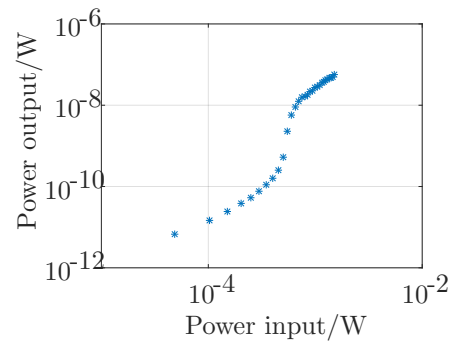


Figure 14: Raw data from the experiment. This is before zooming in on a small wavelength interval. The data is from the cavity L_{15} , to showcase the number of modes, shown by the number of spikes in the dataset. The input power is 804 mW. The peak chosen would in this situation be the one at 1590 nm. The large peak to the left is reflected light from the pumping laser.



(a) The measurements of the L_{10} cavity, in an absolute plot.



(b) The measurements of the L_{10} cavity, in a log-log plot.

Figure 15: The output power from the tallest spike of the measurements at 1550 nm.

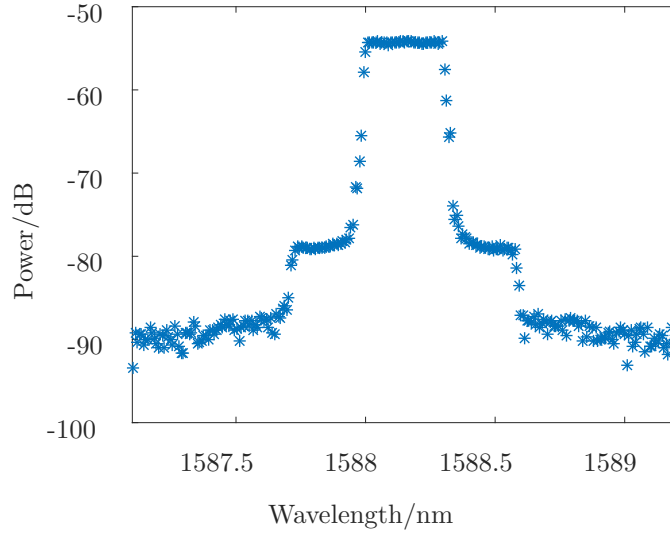


Figure 16: Data from 804 mW. The highest value of the power output is chosen for the experimental data. The shape of the curve is because of the resolution of the detector.

the end the goal will be to fit the simulation to a series of measurements, and hopefully give an estimate of the parameters involved, particularly the β_{sp} -factor.

Plotting the results of the simulation will give a rather flat graph near origo. This graph will make a sharp bend as soon as the input power P_{in} passes the power threshold P_{th} , as shown in Figure 17.

η_i and η_{eff} are both simple efficiency parameters. η_i is an injection efficiency, taking into account all the energy lost between the power meter, and in the photonic crystal. The major contributions to this efficiency are the beam area and light absorption of the crystal. η_{eff} are all the losses starting once the photons leave the cavity, until they are collected. The major contributions to this are the internal losses and the collection efficiency.

Graphically this means changing either of them in the simulation will simply shift their corresponding axis with the same factor, the x -axis for η_i and the y -axis for η_{eff} . Similarly changing V , V_p or rather, the relation between them, Γ , will result in both the x and y -axis being shifted by the same factor as Γ . To get a sense as to why, we need to look at the impact of Γ . In the simulation, we have locked V_p and defined $V = V_p \Gamma$. We see in Eq. (4.1) that the input increases with an increase in carrier volume. Physically, we have to remember that N describes a carrier *density*. Since each carrier requires the same energy to create, and by increasing to total amount of carriers, the input power required for the same N is increased, which will increase the power threshold. The change in the output power is a consequence of the change in the input power, as can be seen in Eq. (4.10). If it takes a higher power to reach the threshold, all the succeeding power calculations will also be shifted by a similar amount.

The two carrier lifetimes, τ_{sp} and τ_{nr} both mainly affect the power threshold P_{th} . Increasing the photon lifetime means increasing the time the carriers stay in the conduction band and make it harder for stimulated emission to happen. This raises the requirement for input energy to reach the threshold, which decreases both P_{th} and g_{th} .

The group velocity v_g interestingly does not matter in regards to the final power output, since the increased number of times each photon bounce on the end mirrors, and the reduced time each photon spends inside the gain material balance out. In regards to N_{th} , only the relation N_{th}/N_{tr} matters since the model for gain, Eq. (3.6), predicts that the bigger the difference is, the larger g_{th} is, thus making the graphs flatter, this is more obvious on the doublelogarithmic plots. g_0 will in a very similar way influence how large g_{th} will be. The β_{sp} -factor makes the curve before threshold steeper, and makes the doublelogarithmic plot flatter, since it makes it so that more photons with the right phase and direction are created independently of stimulated emission.

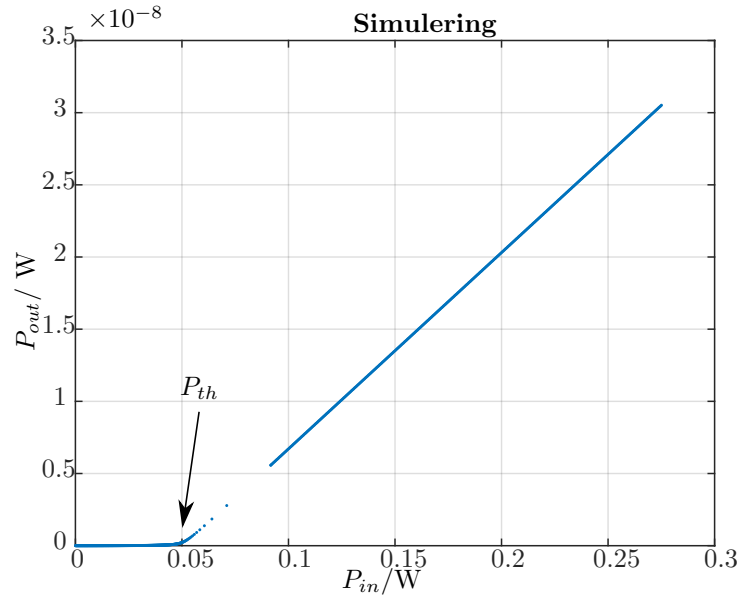


Figure 17: The simulated data shows a clear breakpoint. This is the threshold P_{th} at which point the lasing will occur and the output power will rise linearly with the input power. This sharp turn is how we determine our threshold.

5.2 Qualification of our estimates

For the efficiencies, we have both an injection and effective collection efficiency. We start by looking at the injection efficiency η_i .

For a start, we look at the pump in Figure 13. We assume the area of the cavity to be described by the length and width found in Eq. (3.11) and (3.12). We have $a = 438$ nm, and the radius of the laser beam to be 10×10^4 nm. We assume the pump will have a homogeneous distribution across the complete pump area. The effective area then becomes

$$\begin{aligned}
 \eta_{area} &= \frac{L_{10}W}{(10 \times 10^4 \text{ nm})^2 \pi} \\
 &= \frac{(\sqrt{3}/2 \cdot 238 \text{ nm} \cdot 22)(\frac{1}{2} \cdot 3\sqrt{3} \cdot 238 \text{ nm})}{(10 \times 10^4 \text{ nm})^2 \pi} \\
 &= 9 \cdot 10^{-5}
 \end{aligned} \tag{5.1}$$

When the pump light hits the crystal, it also has to be absorbed. This efficiency is estimated to be 0.002, see Appendix G.

For the output efficiency, we look primarily at the collection efficiency at about 20%. This is due to the photonic crystal laser emitting the light in all directions. This is the only quantitative output efficiency we have and we still lack several orders of magnitude. Some contributing factors could be impurities in the photonic crystal, the internal loss, the mirror losses with others.

It should be said, that many of the parameters can influence things that other can, too. We simply have too many degrees of freedom to determine all the parameters accurately. The only factor that seems to be determinable is the β_{sp} factor.

Using the area efficiency calculated in Eq. (5.1), the absorption efficiency of 0.002, it is possible to calculate the injection efficiency to $\eta_i = 0.0064$

For the effective lasing, the only estimate we have is the collection efficiency of 20%, but we ended up being off by about a factor 10^2 to get the power we see in the results. The efficiency used is $\eta_{eff} = 7.9 \times 10^{-3}$. As stated earlier, however, the Γ -factor will shift the plot on both the x and y axis. This means that we have 3 degrees of freedom, but only two controlling parameters. To

get around this problem, we let η_i be a constant in the simulation, and count on the calculated efficiency (based on the beam area and absorption), and vary η_{eff} and Γ in the simulation. Our way of determining the P_{th} is by finding the starting point of lasing, and see the power input, see Figure 17.

5.3 Fitting simulation to data

A lot of the variables in the rate equations can be expressed in terms of other variables, which reduces the tweakable parameters somewhat. One notable exception to this is the photon lifetime τ_p , where it was earlier approximated by Eq. (4.5) this approximation relies on β_{sp} being relatively small. Since we expect the β_{sp} to be quite large for our laser this is no longer a good approximation. By applying our guesses as well as tweaking the remaining independent variables it is possible to fit the simulation to the measured numbers, and thus getting at least an idea of the magnitude of the β_{sp} factor of the photonic crystal laser.

The list of parameters for the simulation of varying current was quite large. For obvious reasons, it is not feasible to fit 12 different parameters for our method of extracting the β_{sp} factor, and other desired values. To simplify this, we unite some parameters. The mirror loss and the average internal loss can be described using Eq. (4.6). This removes the requirement to approximate the internal loss, the reflectivities, and the reflectivities at the end of the cavity. The reflectivities do not make sense in this context either, because we are working with a photonic crystal laser where the output is measured above the cavity. While the rate equations (and therefore the simulations) are the same for the two, a couple of parameters do not physically make sense in the photonic crystal laser.

Using Eq. (4.7) to convert the photon density to power output, we can see more parameters which no longer impact the simulation. Two of the more interesting parameters which do not impact the power output are the g_0 and v_g factors. To examine why this is the case, we take a look at the steady state solutions found in Eq. (4.1) and Eq. (4.2). While the steady state for the current is paraphrased to power input and the photon density is paraphrased to output power, they both *originally* depend on the material gain and group velocity. We take a look at the input power. As explained earlier in section 4.1, we calculate both gain, output, and input in the stated order. To examine the input, we have to look at the output, too

$$\frac{\beta_{sp} \frac{N}{\tau_{sp}}}{v_g(g_{th} - g)} \quad (5.2)$$

multiplied by the last term of the input in Eq. (4.1) we get

$$\begin{aligned} v_g g N_p &= \frac{g \beta_{sp} \frac{N}{\tau_{sp}}}{g_{th} - g} \\ &= \beta_{sp} \frac{N}{\tau_{sp}} \left(\frac{g}{g_{th}} - \frac{g}{g} \right) \\ &= \beta_{sp} \frac{N}{\tau_{sp}} \left(\frac{g_0 \log \frac{N}{N_{tr}}}{g_0 \log \frac{N_{th}}{N_{tr}}} - 1 \right). \end{aligned} \quad (5.3)$$

As it can clearly be seen, the only term in the power input with the group velocity and gain will cancel out, and the factors therefore do not impact the input power.

To examine the output power, we have to look at the photon density and the factor to get the power output.

The conversion factor is given by Eq. (4.7) and the photon density is given by the same as before. Thus, the output power becomes

$$\begin{aligned} V \beta_{sp} \frac{N}{\tau_{sp}} \frac{g_{th}}{g_{th} - g} \\ = \beta_{sp} V \frac{N}{\tau_{sp}} \left(1 - \frac{g_0 \log \frac{N_{th}}{N_{tr}}}{g_0 \log \frac{N}{N_{tr}}} \right). \end{aligned} \quad (5.4)$$

What we finally see, is the information of the photon lifetime is included in the threshold for the carriers and the gain and group velocity is included in the transformation to power output. The photon reservoir volume was calculated. By varying Γ instead of V , we get a more tangible value.

The ε is used to model the gain, as can be seen in Eq. (3.6). The gain is not completely independent from the input power, as can be seen in the denominator. With more photons, the gain will slowly decrease. If the pump power is far bigger than the power threshold ($\approx 10 \times P_{th}$), the gain will begin to decrease. Because our measurements only go to $\approx 3 \times P_{th}$, it is not a bad approximation to let $\varepsilon = 0$.

In the end, the following significant values were found:

$$\tau_{sp} = 1 \cdot 10^{-9} \text{s}^{-1}$$

$$\tau_{nr} = 1 \cdot 10^{-1} \text{s}^{-1}$$

$$N_{tr} = 1.7 \cdot 10^{24} \text{m}^{-3}$$

$$\varepsilon = 0 \text{m}^3$$

$$\eta_i = 6.4 \cdot 10^{-3}$$

$$\eta_{eff} = 7.9 \cdot 10^{-3}$$

$$\Gamma = 0.01$$

$$\beta_{sp} = 0.25$$

Plotting the resulting graph vs. the measured results can be seen in Figures 18a and 18b, with the measurements being shown as red stars and the simulation result being shown as blue dots.

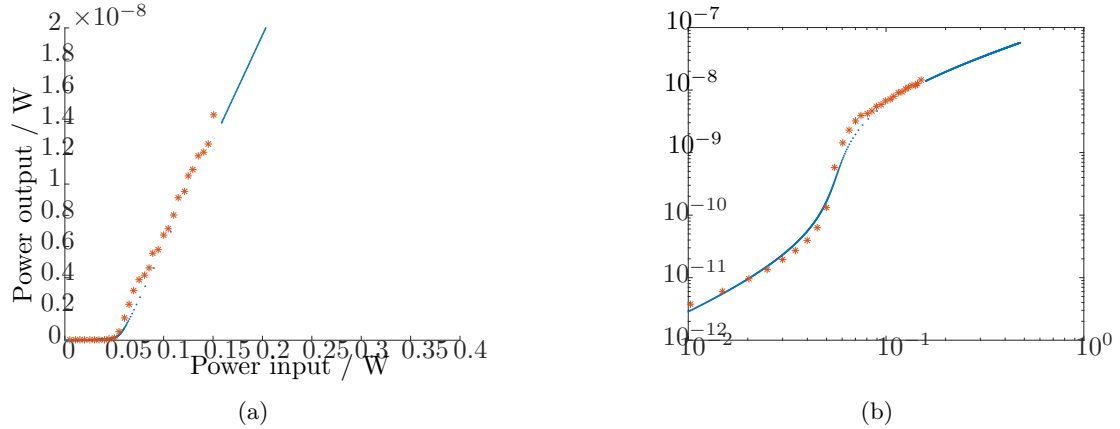


Figure 18: Normal and doublelogarithmic plot of $P_{in} - P_{out}$ curves of the L_{10} photonic crystal structure. Orange stars represent experimental data, and blue circles represent simulation of the rate equations. Most notably, the $\beta_{sp} = 0.25$ fits well.

As expected the β_{sp} -factor is quite large, 25% of all spontaneous emissions have the right phase and direction to add to the photon reservoir. This reflects that there is a limited number of modes possible for the spontaneous emission to decay into, limited by the photonic bandgap formed by the photonic crystal itself. The value is not unusually high for a photonic crystal laser. Other measurements of photonic crystals have shown a β_{sp} -factor of the same magnitude.[6] [5]

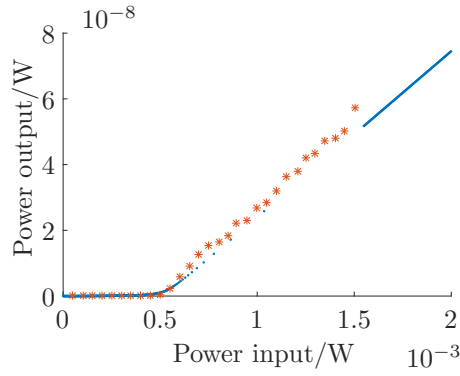
6 Commercial Laser

For the sake of comparison, a commercial laser was also tested, with the intent to give an estimate of the β_{sp} -factor. The laser was of the model FOL1404QQO. The manufacturer's specifications of

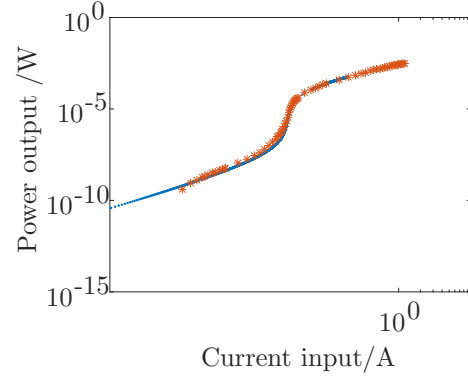
the laser can be seen in Appendix F. This is the same laser used to pump the photonic crystal laser, seen in Figure 12. Given that the commercial laser uses a semiconductor as gain medium, it is expected to have a significantly smaller β_{sp} -factor compared to the photonic crystal laser.

The setup used to make the measurements are the same as the one for the photonic crystal laser, but instead of comparing input power from the pump laser to the output power by measuring the peak intensity of the wavelength were looking for, we compare the input power of the power supply with the output of the pump laser bypassing the attenuator.

The measurements are made by slowly raising the input current of the laser, and measuring the output power. The same simulation used for the photonic crystal laser is used here except we do not convert the input current to power. The laser used had a wavelength of $\lambda = 1480\text{ nm}$. As discussed in section 5.3, many of the parameters influence each other, and it is hard to make the simulation because of too many degrees of freedom. The data and simulation can be seen in Figures 19a and 19b.



(a) Simulation of the commercial laser with variables put in.



(b) simulation of the commercial laser with variables put in, on a doublelogarithmic scale.

Figure 19: Comparison between measured and simulated data for a FOL1404QQO-laser.

The final parameters used to achieve this simulation look as follow:

$$\begin{aligned}
 \eta_i &= 0.8 \\
 \eta_{eff} &= 5.1 \cdot 10^{-3} \\
 V &= 4.8 \cdot 10^{-12} \text{ m}^3 \\
 V_p &= 1.5 \cdot 10^{-10} \text{ m}^3 \\
 N_{th} &= 10^{25} \text{ m}^{-3} \\
 N_{tr} &= 10^{24} \text{ m}^{-3} \\
 \tau_{sp} &= 5 \cdot 10^{-4} \text{ s}^{-1} \\
 \tau_{nr} &= 10^{-3} \text{ s}^{-1} \\
 \beta_{sp} &= 4 \cdot 10^{-4}
 \end{aligned}$$

As expected the β_{sp} -factor of the commercial laser is significantly smaller than the β_{sp} -factor of the photonic crystal laser. The volumes of the carrier- and photon reservoir, V and V_p , and the injection- and collection efficiencies η_i and η_{eff} , are educated guesses based on a similar laser using a semiconductor as gain medium. [1]

Although these numbers are not very accurate, they do give an idea of the approximate sizes of the parameters of the laser, from this we see that, as expected, the β_{sp} -factor of the commercial laser is significantly smaller than the one of the photonic crystal laser.

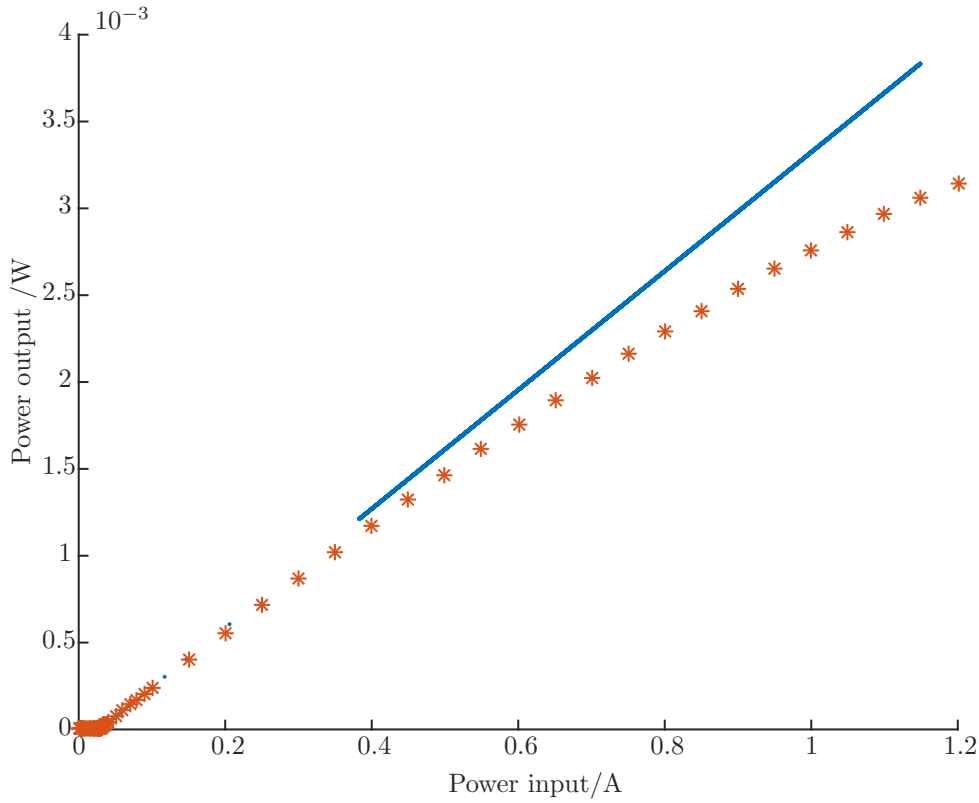


Figure 20: Plot of the input current versus the output power. The orange stars represent the experimental data and the blue dots represent the simulated rate equations. The output power clearly diverge from the expected power attained from the simulation. This could be explained by the exclusion of the ε factor, which decreases the gain with an increased photon density. For simplicity's sake, ε has been set to 0. A zoomed in plot at the threshold can be seen in Figure 19a.

7 Discussion of the results

Although it was possible to reproduce the empirical data using the simulation based on the steady state solutions of the rate equations, we saw some large diverging tendencies for the commercial laser when the input current reached $\approx 10 \times I_{th}$, as can be seen in Figure 20.

The mathematical explanation can be seen in Eq. (3.6). When the photon density increases, $1/(\varepsilon N_p)$ becomes smaller and the gain also decreases. This means the rate of new photons decreases with increasing input current.

Because of the already high amount of parameters to determine, and the limited time available, it was prioritised to not focus on the treating of ε , which could make the model better for higher photon densities. The focus of the project has been to extract the β_{sp} -factor, which does not depend on ε .

Unfortunately, ε was not the only parameter which could not be determined. The simulation used far too many parameters, compared to the information that could be extracted from the experimental data. With too many degrees of freedom, it is not possible to say if any other parameters are in the right order of magnitude, except for β_{sp} . The β_{sp} -factor for the photonic crystal was found to be 25% while it was found to be 0.04% for the commercial laser. This is because a higher value of the β_{sp} -factor makes the jump from spontaneous emission to lasing smaller. The β_{sp} -factor is therefore quite accurate, at least in the order of magnitude compared to the other parameters.

Also as expected, the β_{sp} -factor is several orders of magnitudes higher for the photonic crystal laser than the commercial laser. This is in line with the idea of the bandgap not allowing all phases and polarisations, increasing the β_{sp} -factor. Because the commercial laser allows all modes and polarisations, we expect a much lower β_{sp} -factor.

8 Conclusion

We found the β_{sp} -factor of our photonic crystal laser to be approximately 0.25. This is significantly larger than the β_{sp} -factor of the semiconductor-laser, where we found a β_{sp} -factor of $4 \cdot 10^{-4}$. Our result of the large β_{sp} -factor of the photonic crystal is also reported in other studies. [5]

This shows that it is possible to utilise a large fraction of the spontaneous emission of the photonic crystal laser, compared to the usual semiconductor laser.

For the sole purpose of finding the β_{sp} -factor of a laser our simulation-comparison method works quite well. However, it relies on estimation on a lot of constants for the simulation, which makes it a bad method to find anything other than the β_{sp} -factor of the lasers. The amount of degrees of freedom in relation to the unknown parameters are not a problem for this study though. This is because the β_{sp} -factor is in large independent of the other parameters in the simulation.

The model used for gain in particular is quite inaccurate, as it is shown clearly in Figure 20. Although this does not matter before threshold, it makes the simulation increasingly inaccurate the further from threshold the input is, meaning the simulation diverges from measured data at high power inputs. Because the β_{sp} -factor is determined as a kind of difference between the power output before and after threshold, this again does not have a big influence. The power output does not reach a significant difference between the simulation and experimental data until about $\approx 10P_{th}$, which means this is not a problem in determining the β_{sp} -factor.

The most obvious way to improve the simulation would therefore be to incorporate the decreasing gain as a function of the photon density. This would be done by introducing the factor ε into the gain model. Because of limited time, this was not possible for this project.

References

- [1] tasksheet DTU course 34051.
- [2] G. R. Gould. The laser, light amplification by stimulated emission of radiation, 1959.
- [3] J. Winn R. Meade J. Joannopoulos S. Johnson. Photonic crystals, 2007.
- [4] M. Masanovic L. Coldren S. Corzine. Diode lasers and photonic integrated circuits, 2012.
- [5] K. Takeda A. Shinya K. Nozaki H. Taniyama M. Notomi K. Hasebe T. Kakitsuka S. Matsuo T. Sato. Ultralow operating energy electrically driven photonic crystal lasers, 2013.
- [6] L. Ottaviano Y. Chen E. Semenova K. Yvind W. Xue Y. Yu og J. Mork. Threshold characteristics of slow-light photonic crystal lasers, 2015.

Appendix A

Steady state script

```

close all
clear all
clc

%----- Parametre -----

%Input efficiencies
eta_i = 0.0064

%Output efficiency
eta_eff = 8.8e-3;

%Constants
q = 1.602e-19;
h=6.629e-34;
c = 3e8;
lambda = 1550e-9;

%Dimensioner of the cavity
L = 8.34502e-6;
V_p=2.039602890e-18; %photon volume, determined from experimental setup

epsilon=0;

%Carrier lifetimes to decay
tau_sp=1e-9;
tau_nr=1e-1;

%The beta factor
BETA_sp=25e-2;

GAMMA=0.01;

N_tr=1.7e24;
Nth=1.715e24;

%Group velocity, does not matter in the simulation.
v_g=1;

%Material gain, does not matter in the simulation.
g_0=1;
%Carrier volume
V=V_p*GAMMA;
gth = g_0*log(Nth/N_tr);
%----- Parameters done -----

%Number of points for the plot
h1 = 200;

%Defining variables
N = transpose(linspace(1e21,Nth,h1));
g = zeros(h1,1);
Np = zeros(h1,1);
P = zeros(h1,1);
Pout = zeros(h1,1);

```

```

%Loop before the threshold
for i=1:h1-1
    %Equations from 5.9 and 5.10 in Corsaine
    g(i) = g_0/(1+epsilon*Np(i))*log(N(i)/N_tr);
    Np(i) = (GAMMA*(BETA_sp*N(i)/tau_sp))/((GAMMA*v_g*gth) - GAMMA*v_g*g(i));
    P(i) = h*c/lambda*V*(N(i)/tau_sp + N(i)/tau_nr + v_g*g(i)*Np(i));
end

% Power increasing slowly to 3*Pth
P(h1:2*h1) = transpose(linspace(P(h1-1),1.8*P(h1-1),h1+1));

%Power after threshold
for i=h1:2*h1
    Np(i) = Np(h1-1) + ((P(i)-P(h1-1)))/(h*c/lambda*V*v_g*gth);
end
%Photon density converted to power output
Pout = V*v_g*gth*Np.*h*c/lambda*eta_eff;
%Input efficiency
P = P.*1/eta_i;
%Loads the experimental data
load('data.mat');

%Makes a loglog plot
loglog(P,Pout, '.',IP,OP, '*')
xlabel('Power_input/W')
ylabel('Power_output/W')
xlim([5*10^(-5);5*10^(-3)])

%Makes an absolute plot
figure
hold all
plot(P,Pout, '.')
plot(IP,OP, '*')
xlim([0;2*10^(-3)])
xlabel('Power_input/W')
ylabel('Power_output/W')
grid on

```

Appendix B

Script for extracting data

```

%Multiplies by 100 to get all the power, multiplies by 10^-6 to go from
%microwatts to watts.
IP = importdata('L10.txt');
OP = zeros(length(IP),1);

for i = 1:length(IP);
    dat = importdata(num2str(i));
    OP(i) = max(dat(:,2));
end
%adds 6 dBm for the losses
OP = OP+6;

%Converts from dBm to watts
IP = IP./10^6;
OP = 10.^(OP/10)*10^(-3);
fin = [IP,OP];

plot(3*10^8./X16(:,1),X16(:,2),'.')

```

```
xlim([1.888*10^(5),1.89*10^5])
xlabel('Frequency_/Hz')
ylabel('Intensity_/dBm')

%Saves the output in a txt file
save('data','IP','OP')
```

Appendix C

The data file called 'L10.txt'. This file contains the input power (μW). The output datafiles can be downloaded here

<https://goo.gl/o3QoQw>

```
48.1
102.3
149.5
202.6
250.5
299.7
347.8
399.7
450
550
598
602
651
699
748
804
852
894
945
997
1050
1100
1150
1209
1253
1298
1350
1405
1449
1503
```

The data file called 'dataComLaser.txt'. This file contains the input current (in μA) versus the output power(mW).

Input	Output
0.001	0.4e-3
0.0013	0.9e-3
0.0016	1.3e-3
0.0019	1.8e-3
0.002	2e-3
0.0023	2.5e-3
0.0026	3.1e-3
0.0029	3.6e-3
0.0033	4.3e-3
0.0036	4.9e-3
0.0039	5.6e-3
0.004	5.8e-3
0.006	10.7e-3

0.008	17.1e-3
0.01	26.9e-3
0.012	41.6e-3
0.014	63e-3
0.016	97.5e-3
0.018	151.1e-3
0.02	232.8e-3
0.021	296.9e-3
0.022	371.6e-3
0.023	0.471
0.024	0.615
0.025	0.801
0.026	1.072
0.027	1.540
0.028	2.307
0.029	3.697
0.03	6.18
0.031	9.29
0.032	12.95
0.033	16.38
0.034	19.80
0.035	23.48
0.036	26.87
0.037	30.22
0.038	33.86
0.039	37.21
0.04	40.34
0.05	74.4
0.06	107.7
0.07	141.3
0.08	174.8
0.09	207.7
0.1	240
0.15	400
0.2	559
0.25	715
0.3	868
0.35	1022
0.4	1170
0.45	1318
0.5	1467
0.55	1610
0.6	1751
0.65	1890
0.7	2028
0.75	2159
0.8	2286
0.85	2411
0.9	2531
0.95	2648
1	2762
1.05	2867
1.1	2965
1.15	3058
1.2	3147

Appendix D

The code, including parameters used to simulate the varying current:

```

clear all
close all
clc

%Parameters
global L CCS MA V V_p GAMMA v_g a_i a_m r_1 r_2 g_0 epsilon N_tr
global eta_i tau_sp tau_nr tau_p BETA_sp q I tf Ith
L=300e-6;
CCS=1.6e-14; %Carrier cross section
MA=5e-13; %mode area
V=L*CCS; %carrier colume
V_p=L*MA; %photon volume
GAMMA=V/V_p;
v_g=3e8/4.2;
a_i=5e2;
r_1=0.32;
r_2=0.32;
a_m=1/L * log(1/(r_1*r_2));
g_0=1.8e5;
epsilon=1.5e-23;
N_tr=1.8e24;
eta_i=0.8;
tau_sp=5e-10;
tau_nr=1e-3;
tau_p=1/(v_g*(a_i+a_m));
BETA_sp=1e-4;
Ith = 0.0141;
I = 1.1 * Ith;
q = 1.602e-19;
tf = 4e-9;

%Timespan and initial conditions
Tspan = [0 tf];
IC = [10^(-8) 10^(-8)];

%The ODE45 simulation
options = odeset('AbsTol', [10^(-30) 10^(-30)]);
[t,y] = ode45(@RateEqs,Tspan,IC,options);

%Saves the current output data
t1 = t;
y1 = y;

%Changes the current input
I = 2 * Ith;

%The initial conditions are changed to the final values from before
IC = [y(length(y),1) y(length(y),2)];

%Runs the simulation
options = odeset('AbsTol', [10^(-30) 10^(-30)]);
[t,y] = ode45(@RateEqs,Tspan,IC,options);

%Plots the figures
figure(1)
plot([t1 ; t+tf], [y1(:,1); y(:,1)], '-')
figure(2)
plot([t1 ; t+tf], [y1(:,2); y(:,2)], '-')
%Includes the gain
g=g_0./(1+epsilon.*y(:,2)).*log(y(:,1)/N_tr);
figure(3)

```

```
plot(t,g,'-')
```

The ODE45 code, filename is 'RateEqs.m'.

```
function dy = RateEqs(t,y)
global L CCS MA V V_p GAMMA v_g a_i a_m r_1 r_2 g_0 epsilon N_tr
global eta_i tau_sp tau_nr tau_p BETA_sp q I

%Defines the differential equation.
dy = zeros(2,1);

%DN;
dy(1) = (eta_i * I)/(q * V) - ((y(1)/tau_sp) + (y(1)/tau_nr)) -
v_g * (g_0/(1+epsilon*y(2)))*log(y(1)/N_tr)*y(2);
%DNp
dy(2) = (GAMMA * v_g * (g_0/(1+epsilon*y(2)))*log(y(1)/N_tr) - 1/tau_p) *
y(2) + GAMMA * (y(1)/tau_sp) * BETA_sp;
```

Appendix E

The script and parameters used to simulate the commercial laser.

```
close all
clear all
clc

%----- Parameters -----

%Input efficiency
eta_i = 0.8;

%Output efficiency
eta_eff = 5.1e-3;

%Constants
q = 1.602e-19;
h = 6.629e-34;
c = 3e8;
lambda = 1480e-9;

Nth = 1e25;
N_tr = 1e24;

L = 300e-6;
%Dimensions of the cavity
V_p = L * 0.5e-6;
V = L * 0.016e-6;
GAMMA = V/V_p;
v_g = 1;

%Material gain
g_0 = 5e4;

epsilon = 0;
tau_sp = 5e-4;
tau_nr = 1e-3;

BETA_sp = 4e-4;

gth = g_0 * log(Nth/N_tr);
```

```

%----- Parametre slut -----

%Number of points for the plot
h1 = 20000;

%Defining variables
N = transpose(linspace(1e21,Nth,h1));
g = zeros(h1,1);
Np = zeros(h1,1);
I = zeros(h1,1);
Pout = zeros(h1,1);

%Loop before th
for i=1:h1-1
    %Equation 5.9 and 5.10 from C&C
    g(i) = g_0/(1+epsilon*Np(i))*log(N(i)/N_tr);
    Np(i) = (GAMMA*(BETA_sp*N(i)/tau_sp))/((GAMMA*v_g*gth) - GAMMA*v_g*g(i));
    I(i) = q*V/eta_i*(N(i)/tau_sp + N(i)/tau_nr + v_g*g(i)*Np(i));
end

%Defines the gain to be constant
gth = g(h1-1);

%Input current slowly increasing
I(h1:2*h1) = transpose(linspace(I(h1-1),3*I(h1-1),h1+1));

%Output photons after th
for i=h1:2*h1
    Np(i) = Np(h1-1) + ((I(i)-I(h1-1)))/(q*V/eta_i*v_g*gth);
end
%Changing photon density to output power
Pout = V*v_g*gth.*Np*h*c/lambda*eta_eff;

%Loads the data file
load('fin.mat');
%Converts data output to watts
OP = OP.*1e-6;

%Plots
hold on
plot(I,Pout,'.')
plot(IP,OP,'*')
hold off
alpha(0.5)
xlabel('Power_input/A')
ylabel('Power_output/W')

figure
loglog(I,Pout,'.',IP,OP,'*')
xlabel('Current_input/A')
ylabel('Power_output/W')
xlim([10^(-4);10])
set(gca,'FontSize',20)

```

Appendix F

Datasheet for the commercial laser, given by the producer.

1480 Pump Laser Diode Module (with Isolator)



Applications

- Pump Source for Er-Doped Fiber Amplifier
 - C- and/or L-Band EDFA
 - Single Channel Amp to DWDM Amp

Product Type :

FOL1402P/1404Q/1405R/1425R/1437R Series

Descriptions

- The FOL14xx series (with Isolator) has been designed for use in a wide variety of optical amplifier, such as EDFA used in optical transmission systems, especially in dense wavelength-division-multiplexing (DWDM) systems.
- A strained multi-quantum well laser diode chip is integrated with thermo-electric cooler (TEC), thermistor and PIN photodiode in a hermetically sealed 14 pin butterfly package.
- A 2-lens-system couples a round shape light from the laser chip efficiently to the fiber and enables the output power up to 500 mW.
- This laser module complies with telecom requirements described in Telcordia™ GR-468 requirement and manufactured in an ISO™9001 certified production line.

Features

- Rated output power up to 500 mW (CW)
- Widely deployed reliable package design with industry compatible 14 pin butterfly footprint
- Internal Thermo-electric cooler (TEC) and Thermistor for stable operation
- Integrated PIN photodiode for back facet monitor
- Internal optical Isolator
- Single mode fiber and Polarization maintaining fiber pigtail
- EU RoHS compliant (Exemption 7(c)-1, 13(a) applied)

FOL14xx Series (with Isolator)

Jul. 2014

Absolute Maximum Rating

Parameters	Sym.	Min.	Max.	Unit
Storage Temperature	Tstg	-40	85	°C
Operating Case Temperature 1402P(see TableA)	Tc	-20	75	°C
1402P(see TableA)		-20	70	
1404Q,1405R,1425R,1437R		-20	70	
LD Forward Current 1402P	If	-	1000	mA
1404Q		-	1300	
1405R		-	1600	
1425R		-	1700	
1437R		-	2100	
LD Reverse Voltage	Vr	-	2	V
PD Forward Current	IfPD	-	5	mA
PD Reverse Voltage	VrPD	-	20	V
TEC Current 1402P	Ic	-0.6	2	A
1404Q		-1.1	4.5	
1405R,1425R,1437R		-1.1	4.5	
TEC Voltage 1402P	Vc	-	4.5	V
1404Q		-	4.2	
1405R,1425R,1437R		-	4.5	

Specifications

(LD Temperature (Ts) = 25°C)

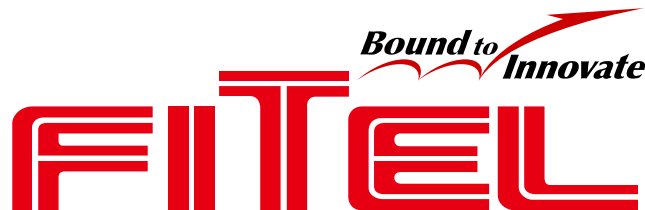
Parameters	Sym.	Min.	Typ.	Max.	Unit	Conditions
Output Power ¹⁾	Pf	Table A			mW	
Forward Current	If					
Center Wavelength(FP)	λ	1460	-	1490	nm	RMS(-20dB), Rated Power
Spectral Width	$\Delta\lambda$	-	-	8	nm	RMS(-20dB), Rated Power
Forward Voltage	Vf	Table A			V	Rated Power
Forward Current at EOL 1402P,1404Q,1405R,1425R 1437R	IfEOL	- -	- -	1.2xIfBOL 1.15xIfBOL	mA	
Monitor Current 1402P 1404Q 1405R,1425R,1437R	Im	50 100 100	- - -	1000 1500 2000	μ A	VrPD=5V, Rated Power
Monitor Dark Current	Id	-	-	100	nA	VrPD=5V
Extinction Ratio	Re	16	-	-	dB	-417 ²⁾
Isolation	Iso	30	-	-	dB	
TEC Specification	-	Table A				
Thermistor Resistance	Rth	9.5	10	10.5	k Ω	Ts = 25°C
Thermistor B Constant	Bth	-	3900	-	-	Ts = 25°C

1) Pf: Available Pf may depend upon center wavelength selected.

2) Design Description (See Table A and Ordering Information for detail)

ODC-DC001B

FOL14xx Series (with Isolator)



Jul. 2014

Part Number	Build-in Isolator	SM fiber	PM fiber
FOL14xxxxx-317	X	X	
FOL14xxxxx-417	X		X

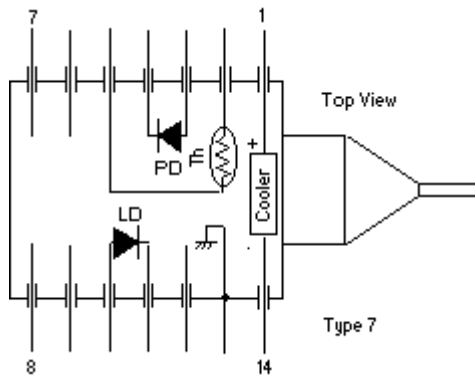
Table A

*:EOL

Part Number	Pf(mW)	If(mA) max	Vf(V) max	Tc(°C)	Itec(A)* max	Vtec(V)* max	Wtotal(W)* max
FOL1402PJX	120	500	2.5	75	1.2	2.7	4.0
FOL1402PJY	130	500	2.5	75	1.2	2.7	4.0
FOL1402PLZ	140	600	2.5	75	1.3	3.0	5.1
FOL1402PLE	150	600	2.5	75	1.3	3.0	5.1
FOL1402PLF	160	600	2.5	75	1.3	3.0	5.1
FOL1402PMG	170	700	2.5	75	1.5	3.5	6.8
FOL1402PMH	180	700	2.5	75	1.5	3.5	6.8
FOL1402PMI	190	700	2.5	75	1.5	3.5	6.8
FOL1402PNJ	200	800	2.5	70	1.7	3.6	7.8
FOL1402PLG	170	600	2.5	70	1.2	2.7	4.4
FOL1402PLH	180	600	2.5	70	1.2	2.7	4.4
FOL1402PMI	190	700	2.5	70	1.4	3.1	5.8
FOL1402PMJ	200	700	2.5	70	1.4	3.1	5.8
FOL1402PMK	210	700	2.5	70	1.4	3.1	5.8
FOL1402PML	220	700	2.5	70	1.4	3.1	5.8
FOL1402PNM	230	800	2.5	70	1.7	3.6	7.8
FOL1402PNN	240	800	2.5	70	1.7	3.6	7.8
FOL1402PNO	250	800	2.5	70	1.7	3.6	7.8
FOL1404QPK	210	900	2.5	70	2.7	2.5	8.7
FOL1404QPL	220	900	2.5	70	2.7	2.5	8.7
FOL1404QPM	230	900	2.5	70	2.7	2.5	8.7
FOL1404QQN	240	1000	2.5	70	3.0	2.7	10.5
FOL1404QQO	250	1000	2.5	70	3.0	2.7	10.5
FOL1404QQP	260	1000	2.5	70	3.0	2.7	10.5
FOL1405RSA	270	1200	2.6	70	2.7	3.4	12.3
FOL1405RSB	280	1200	2.6	70	2.7	3.4	12.3
FOL1405RTC	290	1300	2.6	70	2.9	3.7	14.1
FOL1405RTD	300	1300	2.6	70	2.9	3.7	14.1
FOL1405RTV	320	1300	2.6	70	2.9	3.7	14.1
FOL1425RTW	340	1300	2.7	70	2.9	3.7	14.1
FOL1425RTX	360	1300	2.7	70	2.9	3.7	14.1
FOL1425RUY	380	1400	2.7	70	3.2	4.0	16.5
FOL1437R40	400	1400	2.3	70	2.6	3.2	11.0
FOL1437R45	450	1600	2.4	70	2.9	3.5	13.0
FOL1437R50	500	1800	2.5	70	3.2	3.8	15.0

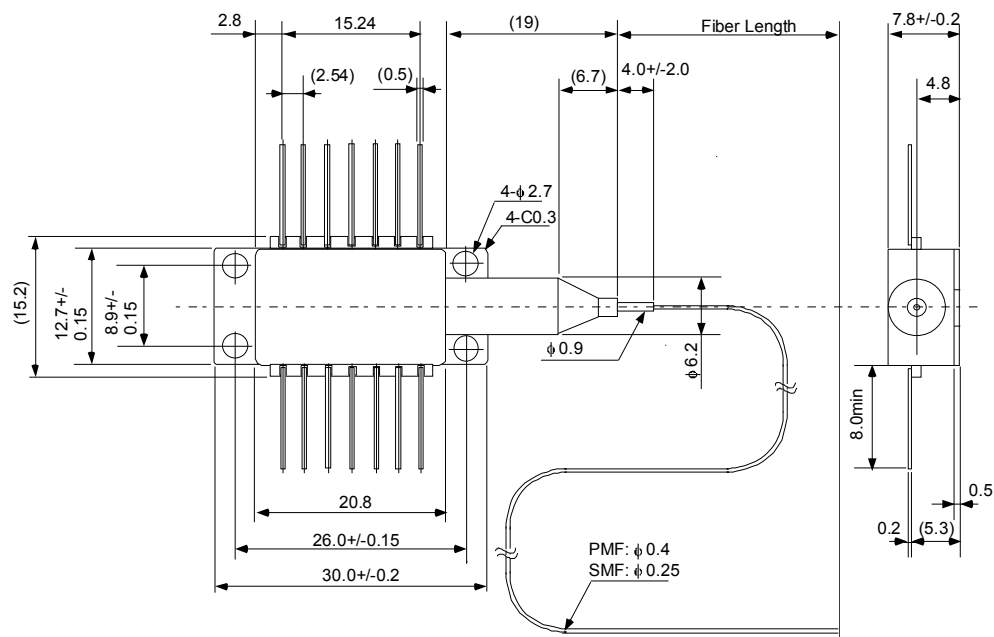
Jul. 2014

Pin Assignment



Pin#	Function	Pin#	Function
1	Cooler(+)	8	No Connection
2	Thermistor	9	No Connection
3	PD anode(-)	10	LD anode(+)
4	PD cathode(+)	11	LD cathode(-)
5	Thermistor	12	No Connection
6	No Connection	13	Case GND
7	No Connection	14	Cooler(-)

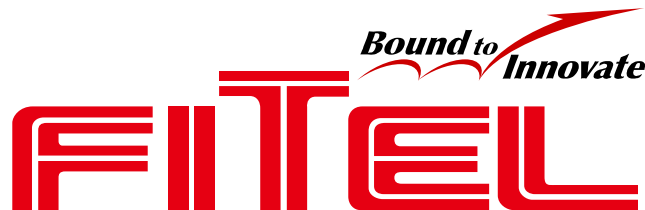
Dimensions

FOL14xxxxx-317 and -417 (w/isolator)

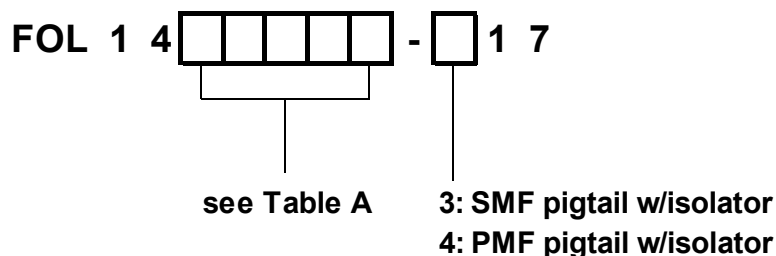
Data Sheet

FOL14xx Series (with Isolator)

Jul. 2014



Ordering information

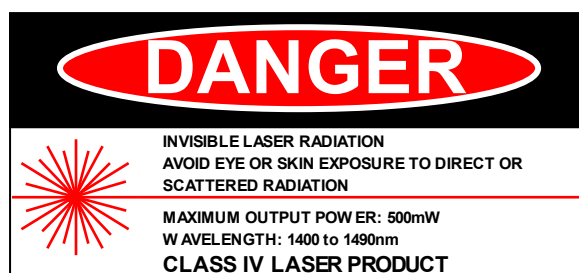


Safety information

This product complies with 21 CFR 1040.10 and 1040.11, Class IV laser product. Invisible laser radiation is emitted from the end of the fiber or connector. Avoid eye or skin exposure to direct or scattered radiation.

ISO is a trademark of The International Organization for Standardization.

Telcordia is a trademark of Telcordia Technologies, Inc.



Furukawa Electric reserves the right to improve, enhance and modify the features and specifications of FITELE products without prior notifications.



Japan
Head Office
2-2-3, Marunouchi
Chiyoda-ku
Tokyo 100-8322, JAPAN
Tel: +81-3-3286-3253
Fax: +81-3-3286-3978
<http://www.furukawa.co.jp>
Email:comsales@ho.furukawa.co.jp

North America
OFS Fitel, LLC
Specialty Photonics Division
25 Schoolhouse Road
Somerset, NJ 08873 USA
Tel: +1-732-748-7402
Fax: +1-732-748-7436
<http://www.SpecialtyPhotonics.com>
E-mail:info@SpecialtyPhotonics.com

Europe
Furukawa Electric Europe Ltd.
3rd Floor, Newcombe House
43-45 Notting Hill Gate
London W11 3FE, UK
Tel: +44-20-7221-6000
Fax: +44-20-7313-5310
<http://www.furukawa-fitel.co.uk>
E-mail:sales@furukawa-fitel.co.uk

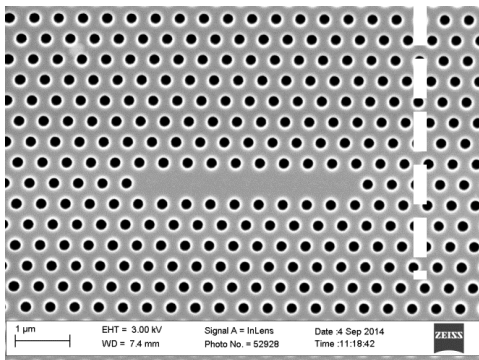
ASIA
Furukawa Electric Hong Kong Ltd.
Suite 2606, Shell Tower,
Times Square, 1 Matheson Street,
Causeway Bay, Hong Kong
Tel: 852-2512-8938
Fax: 852-2512-9717
<http://www.fehk.com.hk/>
E-mail: guest@fehkc.cn

Appendix G

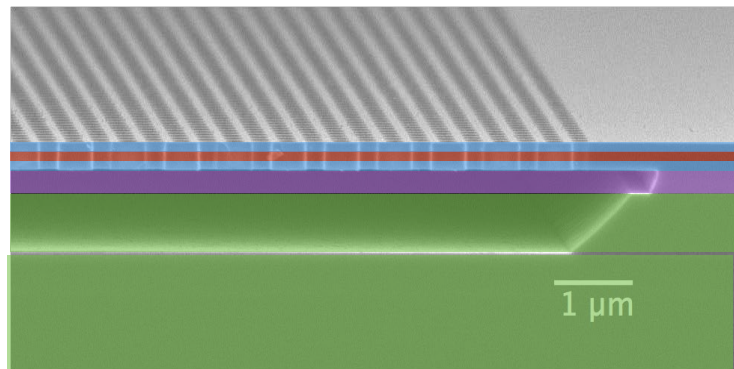
The description given by supervisor Weiqi Xue about the photonic crystal laser.

Structure parameters

Top view



Cross-section view at the dashed line



PhC structure: lattice constant $a_x=438$ nm; air-hole radius 95 nm; membrane thickness 250 nm

Mode volume: length $(N+1)a_x$; Width $2a_y$; Height 250 nm

$$a_y = \frac{\sqrt{3}}{2} a_x$$

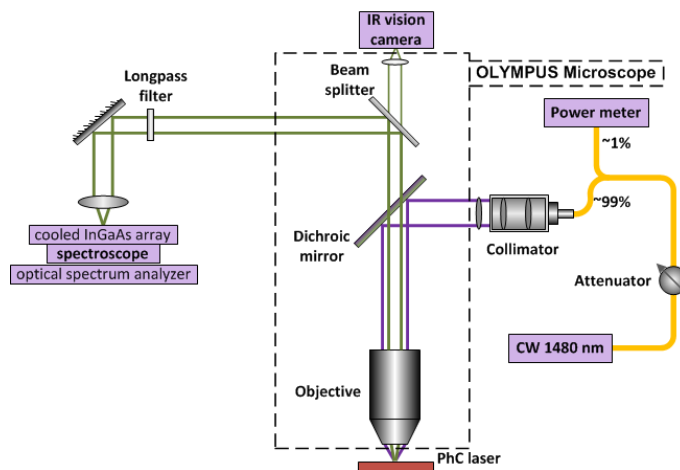
Reflection at the ends: $R=0.94\sim 0.98$

Gain Materials - 3 QD layers

Absorption efficiency: 0.2% (estimated)

Material Gain: unknown (try to play around, a best starting point will be 500 cm^{-1})

Measured emission Spectra from a L9 PhC cavity



The characterization set-up is shown by the figure.

- Each 'txt' file includes the original data of measured emission spectrum at a given pump level. The file name is given by the number shown from the power meter (in μW). There are two columns in the file, the left one for wavelength (in nm), right one for power (in dBm).
- The total transmission loss from the collimator, dichroic mirror and objective is ~ 6 dB.